Performance benchmark of state-of-the-art lateral path-following controllers

Lu, Zhenji; Shyrokau, Barys; Boulkroune, Boulaid; Van Aalst, Sebastiaan; Happee, Riender

DOI
10.1109/AMC.2019.8371151

Publication date
2018

Document Version
Final published version

Published in
Proceedings - 2018 IEEE 15th International Workshop on Advanced Motion Control (AMC 2018)

Citation (APA)
Lu, Z., Shyrokau, B., Boulkroune, B., Van Aalst, S., & Happee, R. (2018). Performance benchmark of state-of-the-art lateral path-following controllers. In Y. Uchimura, & K. Ohishi (Eds.), *Proceedings - 2018 IEEE 15th International Workshop on Advanced Motion Control (AMC 2018)* (pp. 541-546). IEEE. https://doi.org/10.1109/AMC.2019.8371151

Performance Benchmark of state-of-the-art Lateral Path-following Controllers

Zhenji Lu
Cognitive Robotics Department
Delft University of Technology
Delft, Netherlands
z.lu@tudelft.nl

Barys Shyrokau
Cognitive Robotics Department
Delft University of Technology
Delft, Netherlands
b.shyrokau@tudelft.nl

Boulaid Boulkroune
Strategic Research Centre Manufacturing Industry
Flanders Make
Lommel, Belgium
boulaid.boulkroune@flandersmake.be

Sebastiaan van Aalst
Strategic Research Centre Manufacturing Industry
Flanders Make
Lommel, Belgium
sebastiaan.vanaalst@flandersmake.be

Riender Happee
Cognitive Robotics Department
Delft University of Technology
Delft, Netherlands
r.happee@tudelft.nl

***Abstract* — Although extensive research has been conducted to design path-following algorithms for automated vehicles, the cross comparison between different path-following controllers is still weakly-analyzed. Therefore, we benchmarked five path-following algorithms to evaluate their performance according to various disturbances like gust wind, drop of road friction coefficient and inaccurate GPS localization. The comparison was carried out in simulation environment between geometrical-based, path controller with preview, LQR, linear MPC and observer-based controller with integral action approaches.**

Keywords — lateral control, path following algorithm, benchmarking, disturbance, simulation

I. INTRODUCTION

Over the past three decades, considerable research on automated vehicles (AV) has been conducted. The extending capability of automation is making autonomous driving a reality in the near future. Three important basic functions of automated driving system are Perception, Planning and Control. Automation starts perception function to perceive the availability of the space to drive in. Based on the input from perception layer, automation can generate feasible reference trajectory for the vehicle to follow. Then the controller calculates the command to the executive parts to follow the reference path.

Extensive research on controlling car-like robotics have laid the foundation for controller development in AV. Recently, several surveys [1-5] have overviewed the developments over the years. With the usage cases of self-driving car developing from highway/rural to urban environment, the requirements of the controllers become higher due to the necessities of more accurate and robust path tracking for collision avoidance and driver/passenger comfort. However, not many research have thoroughly compared performance of different controllers [4]. This paper focuses on the developments and comparison of controllers for the lateral motion.

Several representative controllers commonly used in automated vehicles path tracking were summarized by several surveys. For tracking based on geometrical model, Stanley method developed by Stanford won the second DARPA Grand Challenge in 2005 [6]. Linear Quadratic Regulator (LQR) control as a basic optimal control method has been widely used in automotive path tracking [2]. Model Predictive Control (MPC) is also being adopted in automotive domain taking advantage of the increasing computing power from the hardware [7-8]. Moreover, an innovative controller Observer-Based Control with Integral action (OBCI), developed by the authors, uses the observer for estimating the internal states to update the controller dynamics [9]. These controllers mentioned above will be used to compared against each other.

Besides testing the tracking accuracy of different controllers in a perfect environment, we also introduced disturbances to evaluate performance of the investigated path-following controllers.

II. VEHICLE SIMULATION MODEL

The 9 DoF simulation model consists of three rigid bodies representing the sprung body, front and rear axles. This model is developed in MATLAB/SimMechanics. The tire dynamics is modelled using Delft-Tire 6.2 with a Magic Formula steady-state slip model describing nonlinear slip forces and moments. The relaxation behavior is linear using empirical relations for the relaxation lengths. The steering dynamics is simplified and represented by a second-order transfer function with time delay and includes Ackerman geometry.

To parametrize and validate the simulation model, experimental tests were conducted using the test platform based on Toyota Prius Gen 3. The test platform is equipped by Spatial Dual Inertial Navigation system from Advanced Navigation and CAN interface for longitudinal/lateral control and data acquisition. The experimental tests cover steady-state and

978-1-5386-1946-9/18/$31.00 ©2018 IEEE

transient lateral vehicle behavior. The experimental tests were carried out on mixed tarmac/concrete surface.

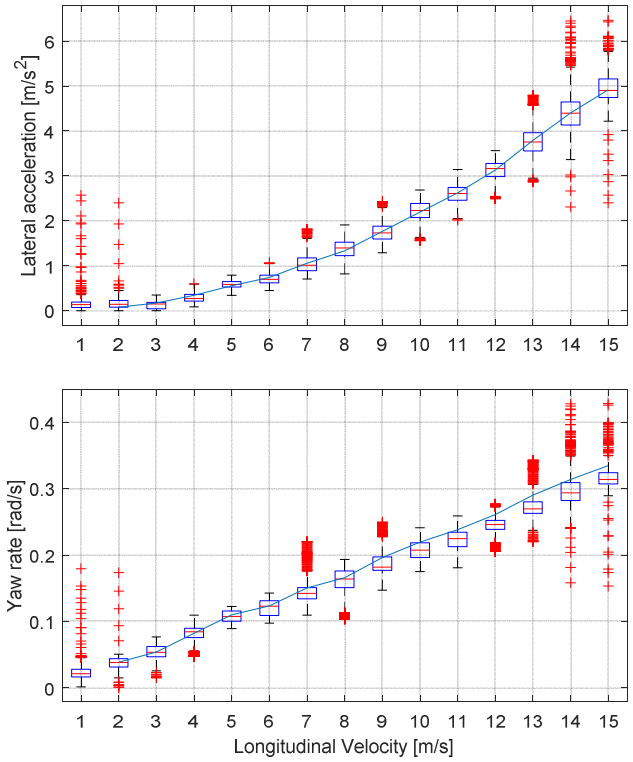

Figure 1 – Steady-state cornering of the vehicle: blue – simulation, red – experimental data

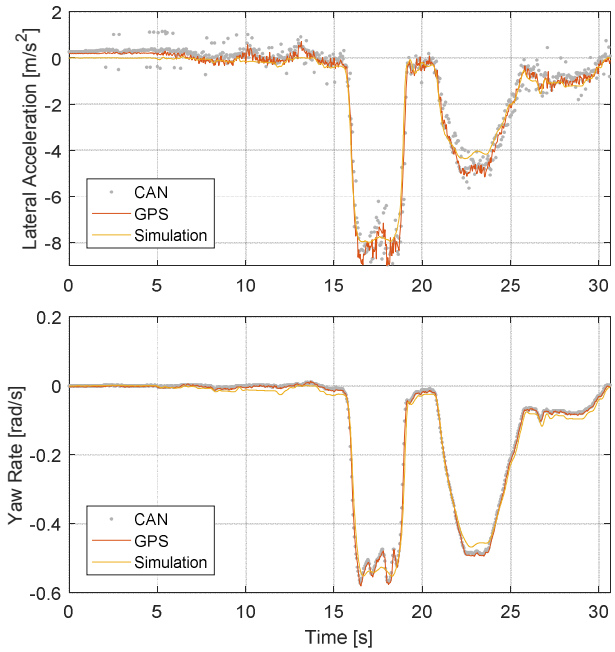

Figure 2 – Transient Step Steer Test

The result of steady-state testing is shown in Fig.1. The experimental data covers left and right cornering with two repetitions for each direction. The steering control was performed by a driver keeping a constant turn radius of 50 m and speed was controlled via CAN interface (slowly increasing from standstill with the longitudinal acceleration of 0.07 m/s^2). Due to a limited test area, the maximum speed reached was around 60 km/h.

The transient lateral behavior was evaluated using Step Steer Tests at 60 km/h with several repetitions. The results of the simulation, GPS and CAN data are shown on Figure 2.

The main vehicle parameters are summarized in Table 1.

Symbol	Table 1 Vehicle parameters		
	Parameter	***Value***	***Units***
m_s	Body mass	1590	kg
m_{us}	Front/rear axles (w/o tires)	85 65	kg
I_{xx}	Body inertia around x-axis	623	kgm^2
I_{yy}	Body inertia around y-axis	2728	kgm^2
I_{zz}	Body inertia around z-axis	2830	kgm^2
l_f	distance from front axle to CoG	1.123	m
l_r	distance from rear axle to CoG	1.577	m
h_{cg}	CoG height above road	0.535	m
B	Front/rear track width	1.519 1.509	m
h_r	Front/rear roll height	0.06 0.15	m
K_r	Front/rear roll stiffness	75200 48800	N/rad
D_r	Front/rear roll damping	3300 2000	Ns/rad
K_z	Front/rear vertical stiffness	52000 48000	N/m
D_z	Front/rear vertical damping	4000 3200	Ns/m
Tire	225/50 R17 (tire property file)		

III. Controller Description

In this section, the path-following algorithms will be described.

A. Stanley

The overall design of the autonomous racing car is presented by Thrun [6], as well as the steering control of it. The steering control is defined as:

$$\delta = e_\psi + \operatorname{atan}\frac{ke_y}{u} \tag{1}$$

As can be seen on Figure 3, δ is the steering angle of the front tires, e_y is the error of distance from the centre of the front wheel to the reference path, u is the speed of the car, k is the gain parameter, and e_ψ is the difference between the orientation angle of the vehicle and the angle of the reference path.

B. Path control with preview (PCFF)

Focusing on the minimization of lateral error and heading error, the control input is defined as [10]:

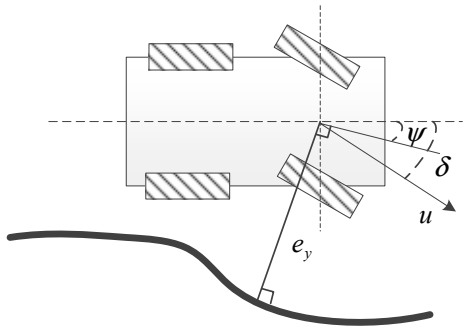

Figure 3 – Stanley model

$$\delta = \frac{2\left(L + K_{us}u^2\right)}{\left(l_r + t_{la}u\right)^2}\left(y_e + t_{la}e_\psi\right) + \delta_{ff} \tag{2}$$

where t_{la} is the look-ahead time; K_{us} is the understeer gradient; L is the wheelbase.

The feedforward contribution is calculated based on the desired yaw rate $\dot{\psi}_{des}$:

$$\delta_{ff} = \left(\frac{L}{u} + K_{us}u\right)\dot{\psi}_{des} \tag{3}$$

C. LQR

The error dynamics model based on the bicycle model is:

$$\dot{x} = Ax + B_1\delta + B_2\dot{\psi}_{des} \tag{4}$$

where state vector $x = (e_y, \dot{e}_y, e_\psi, \dot{e}_\psi)$, and e_ψ is the error of the yaw angle of the vehicle compared to the reference path. δ is the steering input. A, B_1 and B_2 are defined [2] as

$$A = \begin{bmatrix} 0 & 1 & 0 & 0 \\ 0 & \dfrac{-\left(c_f + c_r\right)}{mu} & \dfrac{c_f + c_r}{m} & \dfrac{l_r c_r - l_f c_f}{mu} \\ 0 & 0 & 0 & 1 \\ 0 & \dfrac{l_r c_r - l_f c_f}{I_z u} & \dfrac{l_f c_f - l_r c_r}{I_z} & \dfrac{-\left(l_f^2 c_f + l_r^2 c_r\right)}{I_z u} \end{bmatrix},$$

$$B_1 = \begin{bmatrix} 0 & \dfrac{c_f}{m} & 0 & \dfrac{l_f c_f}{I_z} \end{bmatrix}^T,$$

$$B_2 = \begin{bmatrix} 0 & \dfrac{l_r c_r - l_f c_f}{mu} - u & 0 & \dfrac{-\left(l_f^2 c_f + l_r^2 c_r\right)}{I_z u} \end{bmatrix}^T,$$

in which m is the vehicle mass m, I_z is the yaw inertia, l_f is the longitudinal distance from c.g. to front tires, l_r is the longitudinal distance from c.g. to rear tires, c_f is the cornering stiffness of front tires and c_r is the cornering stiffness of rear tires.

With full state feedback, the control law is defined as:

$$\delta = -Kx \tag{5}$$

To get the optimal δ*, K can be achieved in :

$$K = (R + B_d^T P B_d)^{-1} B_d^T P A_d \tag{6}$$

Minimizing the objective function:

$$J = \sum_{k=0}^{\infty} x^T(k) Q x(k) + \delta^T(k) R \delta(k) \tag{7}$$

D. MPC

By discretizing the model in discrete space as:

$$x_{k+1} = A_d x_k + B_{1,d}\delta_k + B_{2,d}\dot{\psi}_{des,k} \tag{8}$$

To ensure smooth tracking of the reference, the objective function is introduced to minimize:

$$J = \sum_{i=1}^{H_p} \left\| x_{k+i} \right\|^2 Q + \sum_{i=0}^{H_c - 1} \left\| \Delta\delta \right\|^2 R \tag{9}$$

Subject to:

$$\begin{aligned} & x_{k+1} = A_d x_k + B_{1,d}\delta_k + B_{2,d}\dot{\psi}_{des,k} \\ & \delta_{\min} \le \delta_k \le \delta_{\max} \\ & \Delta\delta_{\min} \le \Delta\delta_k \le \Delta\delta_{\max} \end{aligned}$$

where H_p and H_c are prediction and control horizons [7-8].

E. OBCI

Considering a linear parameter-varying system [10]

$$\begin{cases} \dot{x} = A(\rho)x + Bu + Dw \\ y = Cx + Ev \end{cases} \tag{10}$$

by introducing an observer

$$\begin{cases} \dot{\hat{x}} = A(\rho)\hat{x} + Bu + L(\rho)(y - \hat{y}) \\ \hat{y} = C\hat{x} \end{cases} \tag{11}$$

and a feedback controller, as shown on Figure 4:

$$u = -K(\rho)\hat{x} - M(\rho)\int (y^{ref} - y) \tag{12}$$

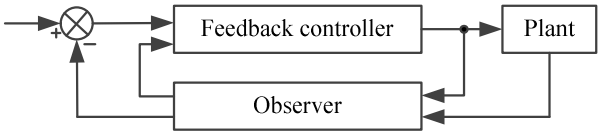

Figure 4 – Schematic overview of OBCI controller

The objective of the controller is to determine the *L(ρ)*, *K(ρ)*, *M(ρ)* by solving sufficient LMI conditions to satisfy the H∞ criterion ensuring the stability of the close loop system.

Transferring a model (4) to (13) to match system format (10):

$$\begin{cases} \dot{x} = Ax + B_1\bar{\delta} \\ y = Cx \end{cases} \tag{13}$$

where $C = \begin{bmatrix} 1 & 0 & 0 & 0 \\ 0 & 0 & 0 & 1 \end{bmatrix}$,

$$\delta = (B_1^T B_1)^{-1} B_1 \bar{\delta} - (B_1^T B_1)^{-1} B_2 \dot{\psi}_{des} \tag{14}$$

IV. Simulation Results

The simulations are carried out using a track profile (Figure 5) and a speed profile (Figure 6). The velocity profile is obtained using an AI driver with following acceleration limits: max. longitudinal acceleration – 1.5 m/s^2; max. longitudinal deceleration – 4.0 m/s^2 and max. lateral acceleration – 5 m/s^2 (linear tire response except friction drop area). The longitudinal velocity for path-following controllers is tracked by a PID controller generating drive and brake torques.

The controllers were tuned to have the best tracking performance of lateral position and heading angle. Their performance is summarized in the Table 1.

Table 1 Path tracking performance

Criteria	Path-following controller				
	Stanley	***PCFF***	***LQR***	***MPC***	***OBCI***
Mean (SD) of lateral error, m	0.11 (0.17)	0.06 (0.10)	0.10 (0.15)	0.09 (0.13)	0.03 (0.04)
Max of lateral error, m	1.17	0.38	0.80	0.73	0.17
Mean (SD) of heading, deg	1.4 (2.0)	0.7 (1.0)	0.6 (1.0)	0.8 (1.1)	0.9 (1.3)
Max of heading, deg	6.4	4.2	4.0	4.2	4.2
Mean steering angle, deg	24.4	24.3	24.4	24.4	24.3

To investigate the performance of the different path-following controllers, the following disturbances are introduced in sections of the track (see Fig 5&6):

- section 1 (red color): gust wind of 15 m/s generating a side force acting on the vehicle CoG;
- section 2 (blue color): drop of road friction from dry asphalt (1.0) to wet asphalt (0.6);
- section 3 (yellow color): random noise with mean of 0.25 m in lateral position representing inaccuracy in GPS localization.

The error of lateral position, the error of heading angle and the lateral acceleration are shown in Figure 7.

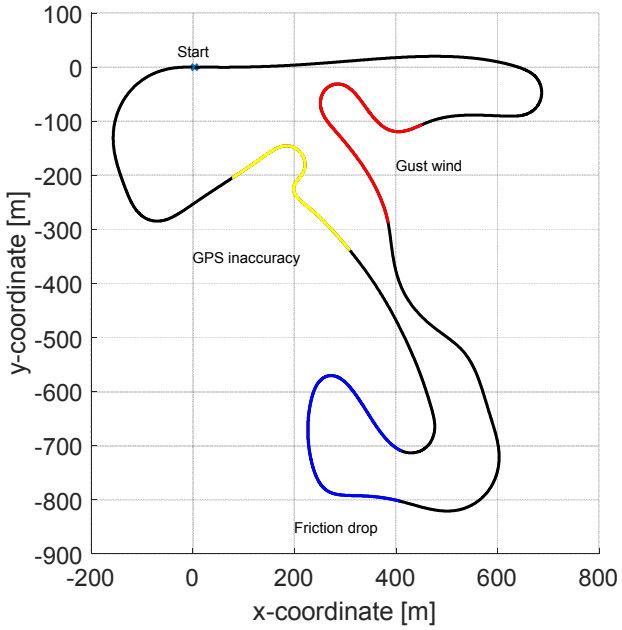

Figure 5 – Track configuration

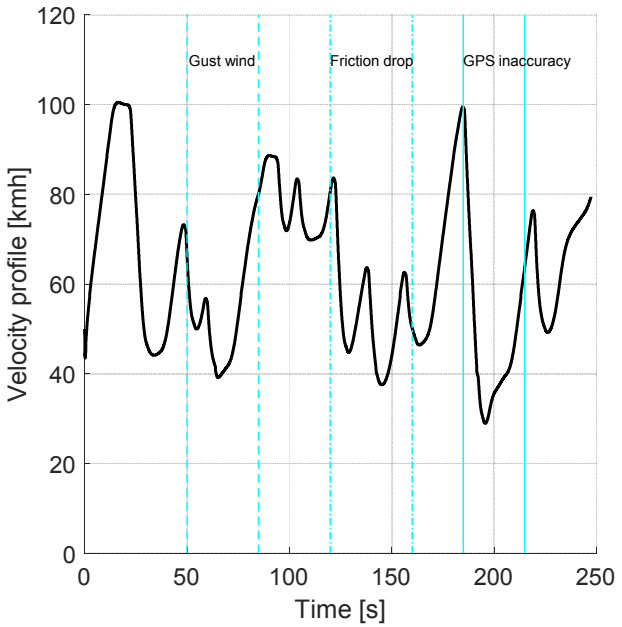

Figure 6 – Longitudinal Velocity profile

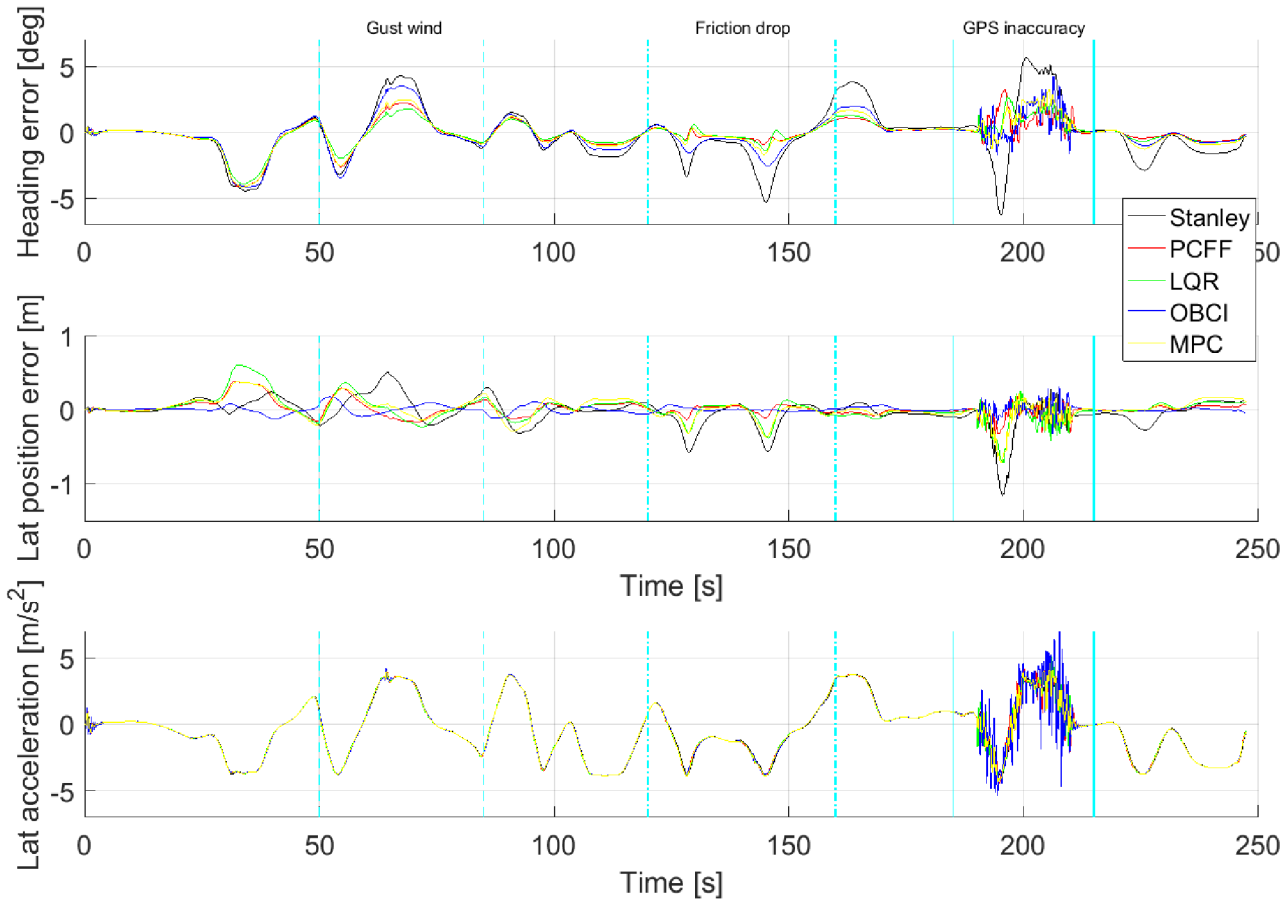

Figure 7 – Tracking performance for the path-following controllers

The tracking performance is summarized in Table 2 for the whole track with three different disturbances scenarios. The key performance criteria were selected to represent tracking performance for lateral and yaw motion as well as required control input.

Table 2 Path tracking performance with disturbances

Criteria	Path-following controller				
	Stanley	***PCFF***	***LQR***	***MPC***	***OBCI***
Whole track					
Mean (SD) of lateral error, m	0.12 (0.19)	0.07 (0.10)	0.10 (0.16)	0.10 (0.14)	0.03 (0.05)
Max of lateral error, m	1.17	0.38	0.72	0.71	0.33
Mean (SD) of heading, deg	1.4 (2.0)	0.7 (1.0)	0.6 (1.0)	0.8 (1.2)	0.9 (1.3)
Max of heading, deg	6.3	4.2	4.0	4.2	4.2
Mean SW angle, deg	24.6	24.6	24.7	24.6	24.8
Section 1: Gust wind					
Mean (SD) of lateral error, m	0.18 (0.21)	0.10 (0.13)	0.13 (0.16)	0.09 (0.12)	0.06 (0.07)
Max of lateral error, m	0.51	0.29	0.36	0.29	0.17
Mean (SD) of heading, deg	0.5 (1.9)	0.3 (1.1)	0.4 (0.9)	0.3 (1.2)	0.2 (1.7)
Max of heading, deg	2.2	1.4	1.1	1.4	2.0
Section 2: Drop of road friction coefficient					
Mean (SD) of lateral error, m	0.15 (0.19)	0.04 (0.05)	0.09 (0.12)	0.08 (0.11)	0.02 (0.02)
Max of lateral error, m	0.58	0.14	0.38	0.37	0.06
Mean (SD) of heading, deg	1.2 (1.6)	0.3 (0.4)	0.4 (0.5)	0.4 (0.6)	0.7 (0.9)
Max of heading, deg	5.3	1.0	1.4	1.7	2.6
Section 3: GPS inaccuracy					
Mean (SD) of lateral error, m	0.21 (0.31)	0.08 (0.10)	0.14 (0.18)	0.13 (0.19)	0.05 (0.08)
Max of lateral error, m	1.17	0.33	0.72	0.71	0.33
Mean (SD) of heading, deg	2.3 (2.9)	0.7 (0.8)	0.7 (0.8)	0.9 (1.0)	0.9 (1.1)
Max of heading, deg	6.3	3.2	2.7	3.2	4.2

In addition, the tracking performance is evaluated for each specific section where the disturbance presents.

The pure kinematic-based path-following controller demonstrates the largest deviation from the reference path and

is sensitive to any kind of disturbance, specifically, GPS inaccuracy.

The path-following controller based on trajectory with preview and feedforward part based on understeer gradient performs well even in the case of disturbance except gust wind.

The path-following controllers based on LQR and linear MPC are capable to provide a sufficient tracking performance; meanwhile, variation of friction conditions (no part of controller system model in the presented study) significantly affect their performance.

With the same model of system dynamics as used in MPC and LQR, The path-following controller based on OBCI demonstrates the best performance as well as the lowest sensitivity to different kinds of disturbance compared to others. Moreover, due to the difficulties of measuring the heading angle and lateral velocity, the OBCI developed does not require full state feedback with the compensations from observer. However, generating feasible solutions of LMI depends on the system dynamics.

V. Conclusion

The proposed study is focused on the benchmark of different state-of-the-art path-following algorithms to evaluate their performance in the case of the different kinds of disturbance like gust wind, drop of road friction coefficient and inaccuracy in GPS localization.

The comparison was carried out in simulation environment between geometrical-based, path controller with preview, LQR, linear MPC and observer-based controller with integral action. To evaluate controllers' performance, a 9 DoF vehicle model validated with experimental tests was used.

Based on the simulation results, it can be concluded that observer-based controller with integral action demonstrates the best tracking performance and less sensitive to different kinds of disturbance compared to other investigated path-following algorithms.

Further work will include experimental tests with the considered path-following controllers.

Acknowledgment

The authors are involved in project I-AT "Interregional Automated Transport" (2017-2021, Interreg, 133141). Special thanks go out to Tom Dalhuisen and Daniel den Hartog for conducting experimental tests, and also to Liang Zhao and Yanggu Zheng for their help with validation of the simulation model.

References

[1] A. Rupp and M. Stolz, "Survey on Control Schemes for Automated Driving on Highways," Automated Driving. Springer International Publishing, 2017, pp. 43–69.

[2] J. Snider, "Automatic steering methods for autonomous automobile path tracking", Robotics Institute, Pittsburgh, PA, Tech. Rep. CMU-RITR-09-08, 2009.

[3] A. Sorniotti, P. Barber, and S. De Pinto, "Path Tracking for Automated Driving: A Tutorial on Control System Formulations and Ongoing Research," Automated Driving. Springer International Publishing, 2017, pp. 71–140.

[4] B. Paden, M. Čáp, S. Z. Yong, D. Yershov and E. Frazzoli, "A survey of motion planning and control techniques for self-driving urban vehicles," IEEE Transactions on Intelligent Vehicles, 1(1), 2016, pp. 33–55.

[5] N. H. Amer, H. Zamzuri, K. Hudha and Z. A. Kadir, "Modelling and Control Strategies in Path Tracking Control for Autonomous Ground Vehicles: A Review of State of the Art and Challenges," Journal of Intelligent & Robotic Systems, 86(2), 2017, pp. 225–254.

[6] S. Thrun et al. "Stanley: The robot that won the DARPA Grand Challenge," Journal of Field Robotics 23(9), 2006, pp. 661–692.

[7] T. Keviczky, P. Falcone, F. Borrelli, J. Asgari and D. Hrovat, "Predictive control approach to autonomous vehicle steering," 2006 American Control Conference, Minneapolis, MN, 2006, pp. 6

[8] P. Falcone, F. Borrelli, J. Asgari, H. E. Tseng and D. Hrovat, "Predictive Active Steering Control for Autonomous Vehicle Systems, " in IEEE Transactions on Control Systems Technology, 15(3), 2007,pp. 566-580

[9] B. Boulkroune, S. van Aalst, K. Lehaen and J. De Smet, "Observer-based controller with integral action for longitudinal vehicle speed control," 2017 IEEE Intelligent Vehicles Symposium (IV), Los Angeles, CA, 2017, pp. 322–327.

[10] A. Schmeitz, J. Zegers, J. Ploeg and M. Alirezaei, "Towards a generic lateral control concept for cooperative automated driving theoretical and experimental evaluation", 5th IEEE International Conference in Models and Technologies for Intelligent Transportation Systems, 2017, pp. 134-139.